WESLEY JAMES
PROF. FRED J. BURGESS
Oregon State University
Corvallis, Oregon 97331

Ocean Outfall Dispersion

Aerial photography offers a possible method for evaluating waste concentrations, dispersion processes, and current patterns.

ABSTRACT: *Aerial photography may provide a method of analyzing dispersion of wastes that are discharged into the ocean. A procedure for determining waste concentrations from aerial photography is described. This technique may yield more comprehensive results than conventional boat sampling in dispersion studies. Discrepancies between boat concentrations and photo concentrations appear to be due primarily to the changing and shifting of the waste in this dynamic environment. The photographic technique is a method of study that may provide information on diffusion which has been impossible to measure by conventional sampling methods.*

INTRODUCTION

OCEAN OUTFALLS ARE in general located on the relatively shallow coastal shelf. Because of heavy seas, sampling from a boat in this near-shore area is dangerous at all times and impossible much of the time. A more effective and less dangerous sampling technique is desirable. The use of aerial photography presents a possible method of overcoming this difficulty. Sampling from a boat to define adequately the waste field for even a small outfall requires from two to eight hours of continuous sampling. Under usual conditions the waste field is continuously changing during this period of time, thus making a comprehensive study of the dispersion by conventional means nearly impossible. This paper attempts to establish a quantitative aerial photographic technique to measure concentrations throughout the waste field which may be recorded as image densities at one instant, thus overcoming many difficulties.

An ocean outfall is a pipeline used for discharging waste into the ocean and it usually terminates with a diffuser section. Here the flow is divided into a number of small jets which discharge into the ambient fluid. If an outfall is located on the coastal shelf in relatively shallow water, usually little density stratification occurs in the receiving body of water. The effluent being less dense than sea water will generally rise to the surface. After the initial dilution in the vicinity of the jet diffuser, the natural turbulence in the ocean continues to mix and spread the waste.

The use of a dye tracer has been the conventional method for studying the dispersion of the waste field from an outfall. In this procedure the tracer is metered into the pipeline on shore. The concentration in the waste field is determined by sampling from a boat and measuring the concentration of the tracer. If the flow rates of both the effluent and tracer are known, the waste concentration can be determined from these samples.

RATIONALE

Photographic films used in aerial photography are sensitive to visible or near-visible light. The film density depends on the irradiance reaching the film. The predominant source of this energy is the sun. Solar radiation passing through the atmosphere is reduced by scattering and absorption. The attenuation depends not only on the turbidity in the atmosphere but also on the length of the path through the atmosphere. The zenith angle i of the sun is involved in reducing the illumination in two ways. First, the intensity on a horizontal surface is cos i times the intensity on a normal plane and, secondly, the path traversed by the radiation through the atmosphere increases with the secant of the

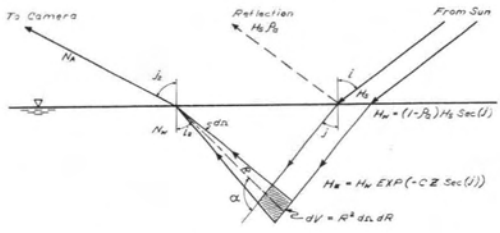

FIG. 1. Light from the sea.

angle. The irradiance H_s on a horizontal plane at the sea surface can be expressed as

$$H_s = H_o \cos i \exp(-A \sec i)$$

where H_o is the incoming radiation at the outer atmosphere and A is the extinction optical thickness for a standard atmosphere and includes Rayleigh attenuation, aerosol attenuation and ozone absorption.[5]

The light reaching the water surface is either reflected from or refracted through the air-sea interface. If i is the angle of incidence and j is the angle of refraction, then (sin i/sin j) is equal to the index of refraction for water, or about 1.33. The reflectivity of the water surface is theoretically obtained for unpolarized light from Fresnel's law[2] which gives the ratio p_a of reflected energy R to incoming radiation H_s. As shown in Figure 1, the irradiance H_w below the sea surface and normal to the beam is

$$H_w = (1 - p_a)H_s \sec j.$$

The radiation that penetrates the surface of the sea is progressively diminished as it travels through the water. By applying Lambert's and Beer's laws for monochromatic light, the intensity $H(z)$ at some depth Z below the water surface is given by

$$H(z) = H_w \exp[-(a + bW)\ Z \sec j]$$

where a is the sea-water attenuation coefficient, b is the waste attenuation coefficient and W is the waste concentration. The minimum attenuation of sea water occurs at about 540 nm (nanometers) whereas the minimum for the waste is about 700 nm. The attenuation coefficients can be divided into attenuation due to absorption and attenuation due to scattering. In solutions with small particles, blue light has the maximum scatter and in solutions with larger particles all colors are scattered about the same amount.

By definition of the volume scattering function $B(\alpha)$, the scattered light intensity dJ from the scattering volume dV in the direction that forms an angle α with the incident beam is

$$dJ = H(z)B(\alpha)dV.$$

For Mie scattering the intensity of the scattered light is proportional to the particle surface area exposed to the incident beam. The intensity of the scattered light is proportional to the waste concentration. The volume scattering function varies with both angle α and the waste concentration. For a vertical photograph taken with an aerial camera with six inch focal length when the sun's zenith angle is 55 degrees, the angle α would vary from about 110 to 170 degrees.

As shown in Figure 1, R is the distance from the volume element dV to the point where the scattered light strikes the surface and $d\Omega$ is the solid angle formed at the surface by dV, then

$$dV = R^2 d\Omega dR.$$

As the intensity of the light which is scattered for the second time is approximately three orders of magnitude less than the direct lighting, the addition of the rescattered light to the emerging ray from the incremental volume will not be considered. The intensity of the emerging ray dJ will be reduced by absorption and scatter of the water and particles. From the inverse-square law, the radiance N_w from the scattering volume at the surface is

$$dN_w = (dJ/d\Omega) \exp[-(a + bW)R]/R^2.$$

Combining equations,

$$dN_w = \frac{H_o \cos i \exp[-A \sec i - (a + bW)(\sec j + \sec i_2)Z]}{\cos i_2 \cos j}[(1 - p_a)B(\alpha)dZ].$$

If the waste concentration is not a function of depth, the resulting equation can be integrated with respect to Z. Letting exp [−(a+bW) (sec j+sec i_2)Z)] approach zero, the equation becomes

$$N_w = \frac{H_o \cos i\ B(\alpha)(1 - p_a) \exp(-A \sec i)}{\cos i_2 \cos j\ (a + bW)(\sec i_2 + \sec j)}.$$

Upon passing through the sea-air interface some light is reflected and the radiance spreads into a larger solid angle.[2]

The radiance from the sea is

$$N_a = \frac{N_w}{n^2}(1 - p_w) \tag{1}$$

where n is the refractive index of water and p_w is the reflectivity at the surface.

The light reaching the camera is composed of sea surface reflection, path luminance in the atmosphere and light from the sea. Assuming the photograph was taken so as to avoid the direct sunlight reflection from the water surface. the surface reflection would be predominantly blue.

Writing Equation 1 for both the red and green light at the sea surface, and taking the ratio N_r/N_g,

$$R = \frac{K_1 B_r(\alpha)(a_g + b_g W)\exp\left[(A_g - A_r)\sec i\right]}{B_g(\alpha)(a_r + b_r W)} \tag{2}$$

where K_1 is a constant and the subscripts r and g refer to the red and green bands, respectively.

The ratio of the volume scattering functions shows the effect of scattering on the composition of the scattered light. As the particle size is relatively large compared to the wavelength of light, the scattered light is of nearly the same composition as the incident light and this ratio is approximately equal to one.

Equation 2 can be rewritten as

$$RA = R\exp\left[(A_r - A_g)\sec i\right] = K_1\frac{a_r + b_r W}{a_g + b_g W}. \tag{3}$$

The term $(A_r\text{-}A_g)$ *sec i* is a constant for a photograph but gives the change in the composition of the incident light as a function of the sun's zenith angle. It is included in the computations so that results from photographs taken at different times will be comparable.

The next several paragraphs will be devoted to developing a relationship between the film density and RA. As shown in Figure 2 let j_2 represent the angle between the ray to the camera and the vertical. Let the angle between the ray and the camera axis be represented by c, then by geometry

$$dA = dA'\left(\frac{Z_0}{f}\right)^2\left(\frac{\cos c}{\cos j_2}\right)^3$$

where dA is the area on the sea surface included in the densitometer aperture area dA' on the photographic film, Z_0 is the flying height and f is the focal length of the camera. The solid angle subtended by the lens of diameter D is

$$d\Omega = \frac{\pi}{4}\left(\frac{D\cos j_2}{Z_o}\right)^2\cos c.$$

The radiant flux dP' collected by the camera lens is

$$dP' = NdA\cos j_2\exp\left[-E\sec j_2\right]d\Omega.$$

The irradiance of the film image[1] is

$$H' = \frac{dP'}{dA'} = \frac{K_2 Tr N\cos^4 c\exp\left[-E\sec j_2\right]}{(FNO)^2}$$

where K_2 is a constant, Tr is the lens transmittance, N is the object radiance at the sea surface, c is the angle between the ray and the camera axis, FNO is the relative aperture (f/D) of the lens, and E is the extinction optical thickness for the attenuation by the atmosphere from the sea surface to the camera.

The photographic exposure EX is a product of image irradiance H' and the duration TIM. The relationship between film density and the exposure is shown by the film's characteristic curve. The curve is a plot of the log exposure *vs* film density for a particular development. If the exposure of the film is on the straight line portion of the curve, then the film density can be expressed by

$$D(x, y) = M + G \ln (EX).$$

D (x, y) is the film density at the point on the photo with film coordinates x and y, M is a constant representing film speed, G is a constant representing film contrast, and EX is the exposure. By combining equations, the radiance from the sea is

$$N_a = \frac{K_3(FNO)^2 \exp\left[D(x, y)/G + E \sec j_2\right]}{TIM\ Tr \cos^4 c}.$$

The ratio of the radiance in the red and green bands is

$$R = K_4 \exp\left\{\left[D_r(x, y) - D_g(x, y)\right]/G + (E_r - E_g) \sec j_2\right\}. \quad (4)$$

Characteristic curves for the films used on the project indicated that the gamma G is nearly the same for the red and green sensitive layers.

Equations 3 and 4 can be combined to give the relationship between the film density and the waste concentration. If R_{ph} is defined as

$$R_{ph} = \exp\left\{\left[D_r(x, y) - D_g(x, y)\right]/G + (E_r - E_g) \sec j_2 + (A_r - A_g) \sec i\right\} \quad (5)$$

and R_{pho} is the value of this ratio when no waste is present, then

$$W = C_1(R_{ph} - R_{pho}) + C_2(R_{ph} - R_{pho})^2 + \cdots \quad (6)$$

where R_{pho} is the ratio determined from Equation 5 for points outside the waste field and R_{ph} is the value from Equation 5 for points within the waste field. A stepwise regression analysis of Equation 6 has shown that only the first two terms on the right are significant.

Field Work

Data utilized for this paper were acquired during the summer of 1968. The general procedure employed in the collection of the data was to take aerial photography of the waste field and simultaneously sample the plume from a boat by conventional procedures.

Accurate control of the positioning of the boat and the orientation of the photography was essential. Concentrations determined from aerial photography were compared to those measured from the boat by matching ground coordinates. To eliminate the possibility of discrepancies in concentration being caused by error in positioning, an accurate control network was established on shore. Also a network of ten photo control buoys was established about the outfall area in such a way that each photo would contain a minimum of three buoys. The position of the buoys and the boat was determined by triangulation from two shore stations. The boat's position while sampling was determined at one-minute intervals.

Rhodamine WT tracer was metered into the pipeline on shore. The concentration of

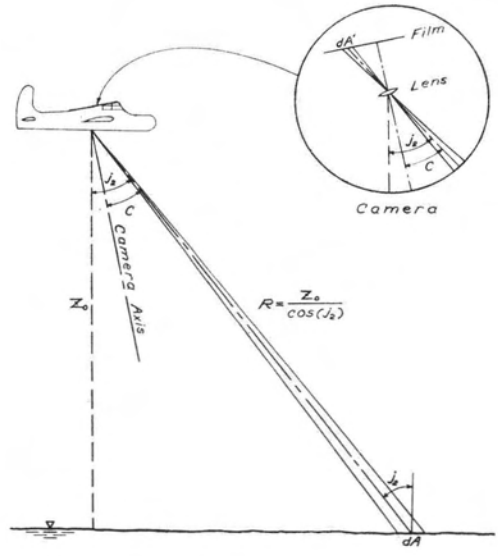

Fig. 2. Geometry of exposure calculation.

this tracer in the waste field was measured by two continuous flow-through fluorometers sampling from two depths. Before photography, floats were set to measure the water currents. The floats were orange in color, four feet square and two inches thick. A drogue was attached to each float.

Photography was taken at two altitudes. Precise mapping cameras and color film were used. The small-scale photography (1:12,000) was intended to be used for buoy location by analytical strip bridging; however, if was found more convenient to triangulate the buoys from shore stations. The low-altitude photography was taken at a scale of 1:6,000. The film was processed with a re-wind film processor.

Reduction of Data

Because of the large volume of data, it was essential that plotting and computations be computerized wherever possible. Boat concentrations were computed and stored on file for comparison with the photo values. Three-dimensional computer plots of the boat concentrations are shown in Figures 3 and 4. The program was revised to include the boat's track in Figure 4. On the plots are several locations within the plume where the concentrations were measured twice at one point. The differences are 4, 2 and 4 units in Figure 3 and 9, 13, 11 and 0 units in Figure 4. These discrepancies in the boat concentrations indicate that the plume had not reached a steady state.

Photographic information was converted to digital data with a photo densitometer. The densitometer was equipped with filters for measuring the density of the three layers of the color transparency. The voltage output of the densitometer went to a digital voltmeter for conversion to BCD. The voltmeter output was wired into an x, y, z digitizer as the z value. An aerial film holder was attached to a coordinatograph for measurement of the x, y photo coordinates. The digitizer was connected to a card punch. One card was required for each point and contained photo identification, point number, x and y coordinates, and densitometer voltages for the three spectral bands of the photograph.

The computer program used for the reduction of photographic data was dimensioned to process information from two flights over the area and up to three photos for each flight. Photographic orientation was accomplished by a non-linear solution to the collinearity condition equations. A published program for resection[3] was modified as a subroutine for this phase of the computations. The position vector based on the state plane coordinate system was determined by multiplying the photographic vector by the inverse of the orientation matrix. The sun's altitude and azimuth were computed from standard surveying formulas. Voltage output

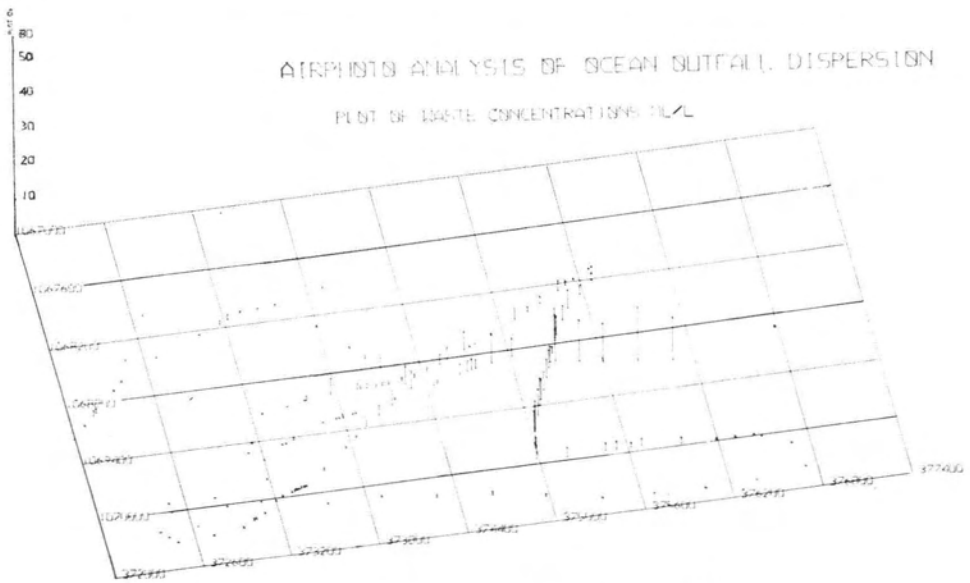

FIG. 3. Plot of boat concentration on August 8, 1968.

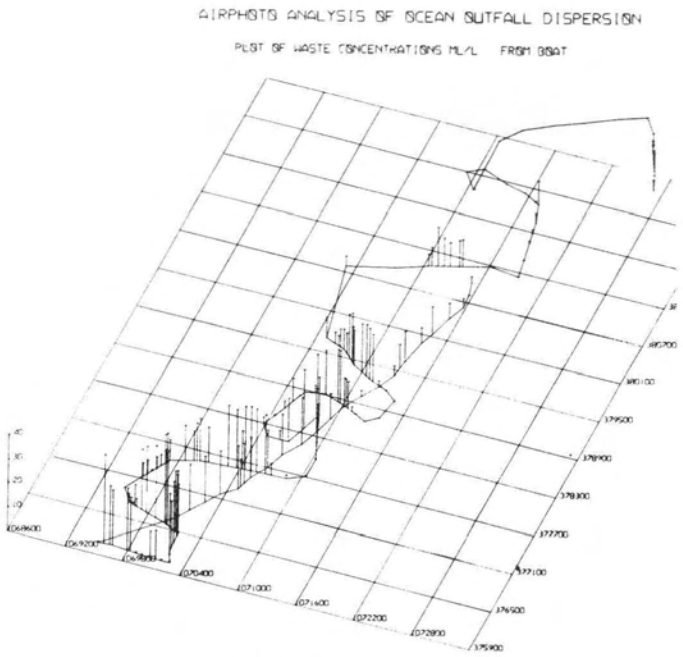

FIG. 4. Plot of boat concentrations on August 16, 1968.

of the densitometer was related to the density by fitting a cubic polynomial to density measurement made on a calibrated gray scale.

Atmospheric attenuation coefficients (A_r and A_g in Equation 5) were determined from Reference 5 for a standard atmosphere. The value of $(E_r - E_g)$ in Equation 5 was approximated by

$$E_r - E_g = -0.024 \ln (Z_0/3280. + 1.)$$

where Z_0 is the flying height in feet. Values of R_{pho} in Equation 6 were determined from the following regression model:

$$R_{pho} = B_0 + B_1(SUNR) + B_2(Nb) + e.$$

The regression coefficients B_0, B_1 & B_2 were determined from a least squares fit of data from points outside the waste field. $SUNR$ is the angle between the ray to the camera and the reflected direct sunlight and Nb is the radiance determined from the blue film density.

Values of $(R_{ph} - R_{pho})$ were computed for each data point on the aerial photos and stored in an array oriented about the waste field. The two indices of the array were related to the ground coordinates of the element. Each element represented a 60-foot square area on the sea. After the film density measurements were converted to $(R_{ph} - R_{pho})$ values, missing values in the array were interpolated from adjacent points.

Boat concentrations were interpolated at 60-foot intervals along the boat's path and matched by ground coordinates with the photo values in the array. A least-squares regression analysis was made on the data with the model

$$W = C_1(R_{ph} - R_{pho}) + C_2(R_{ph} - R_{pho})^2 + e \quad (7)$$

where W is the waste concentration in milliliters per liter and C_1 and C_2 are regression coefficients. Comparisons of waste concentrations measured from the boat with those determined from Equation 6 are shown in Figures 5 and 6.

Listed in Table 1 are the values of the regression coefficients in Equation 7 and their standard error. It can be seen from the table that on August 8 C_2 was generally the most significant in the relationship between the waste concentration and $(R_{ph} - R_{pho})$, whereas on August 16 C_1 was the most significant. During the first day, the tracer concentration was four times as large as in the second day and was visible to the eye. The coefficients for the high-altitude photography are larger than those for low-altitude photography because of contrast attenuation caused by light path radiance. The standard errors of the waste concentration listed in

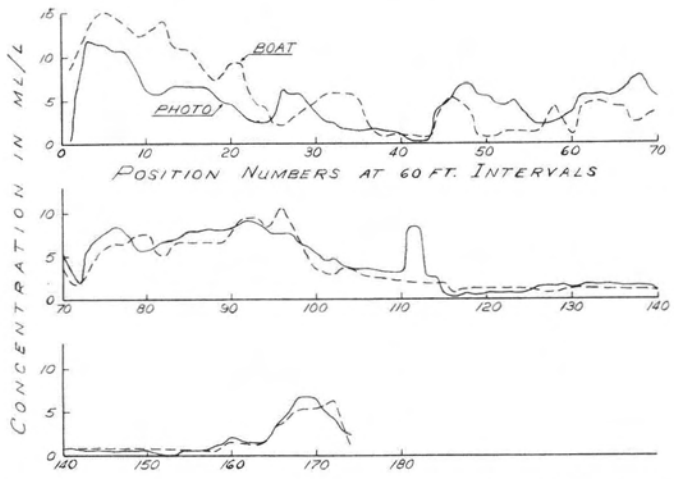

Fig. 5. Comparison of boat and photo concentrations August 8, 1968.

Table 1 are significantly less than the discrepancies within the boat concentrations at a 95 percent confidence level. The boat values are subject to larger variations as they represent the concentration for a point whereas the photo values represent the concentration for a volume. The correlation coefficients between the boat and photo concentrations ranged from 0.88 to 0.91.

After the coefficients in Equation 7 are determined, waste concentration throughout the array are computed. These are displayed as a symbolic plot on the line printer. Figure 7a shows a plot from photographs taken August 8 and Figures 8a and 8b show two plots from photographs taken August 16. The symbols represent different ranges in concentration and were selected so that the density on the plot increases with the concentration.

The plot in Figure 7b was made on the computer controlled calcomp plotter from the data shown in Figure 7a. The symbolic plot from the line printer is distorted as the longitudinal scale is larger than the lateral scale.

Once the concentrations in the plume are known, diffusion coefficients are computed throughout the waste field. One-dimensional, steady-state diffusion coefficients are determined from each set of photos covering the field. The non-steady state diffusion coefficients are determined by comparing concentrations computed from two flights over the area.

Figure 8c is a plot of the concentrations

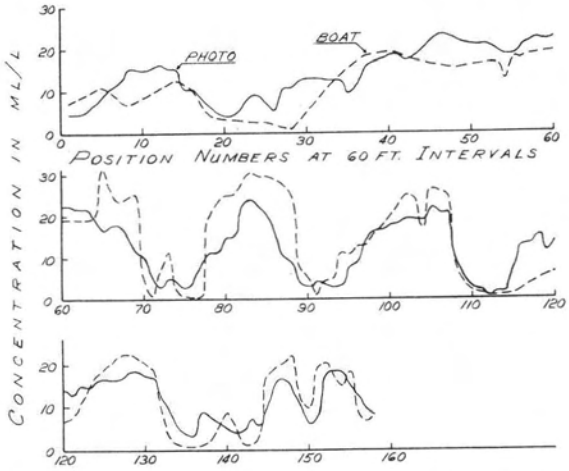

FIG. 6. Comparison of boat and photo concentrations August 16, 1968.

TABLE 1. STATISTICAL ANALYSIS OF PHOTO CONCENTRATIONS

Day	*Time*	*Scale*	*Photo No.'s*	C_1*	C_2*	*Standard Error*			*Deg. Free.*
						C_1	C_2	W	
Aug.	17:21	1:6,000	11, 12	(−0.8)	374	7	55	2.3	172
8	17:31	1:6,000	18, 19	(−6.7)	424	8.2	69	2.7	195
	17:42	1:6,000	25	58.3	425	12.8	167	2.7	142
Aug.	15:52	1:12,000	3, 4	195	(746)	35.5	493	6.2	178
16	16:00	1:6,000	10, 11	146	(205)	21.9	219	5.6	156
	16:14	1:6,000	17, 18, 19	120	(416)	26.6	274	6.3	187

*( ) indicates that the coefficient does not significantly reduce the error.

shown in Figure 8a minus those shown in Figure 8b. Areas on the plot having differences greater than six units were cross-hatched. The outlines of the plumes are also sketched on this plot. It can be seen that the plume had changed considerably during this 22 minute period between the flights. The mean difference in concentrations for this comparison was 1.8 units with an absolute mean of 4.6 and a standard deviation of 5.9 units. The comparison was based on 2,485 points within the plume of each flight. As the concentration gradients were high, a small change in the plume position resulted in a relatively large apparent discrepancy in concentrations.

SUMMARY

The conventional method for measuring the dispersion of waste from an ocean outfall is by sampling from a boat. Because the outfalls are generally located on the relatively shallow coastal shelf, field work in this nearshore area is impossible much of the time because of rough seas. Aerial photography offers a possible method for evaluating waste

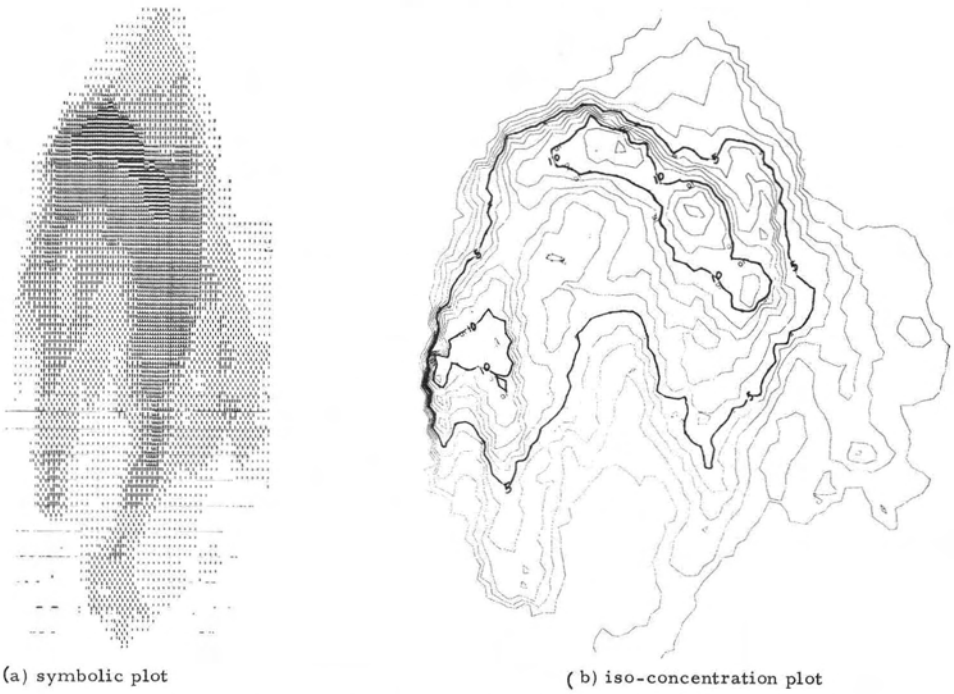

(a) symbolic plot

(b) iso-concentration plot

FIG. 7. Waste concentrations from aerial photography August 8, 1968. (*a*) Symbolic plot. (*b*) Iso-concentration plot.

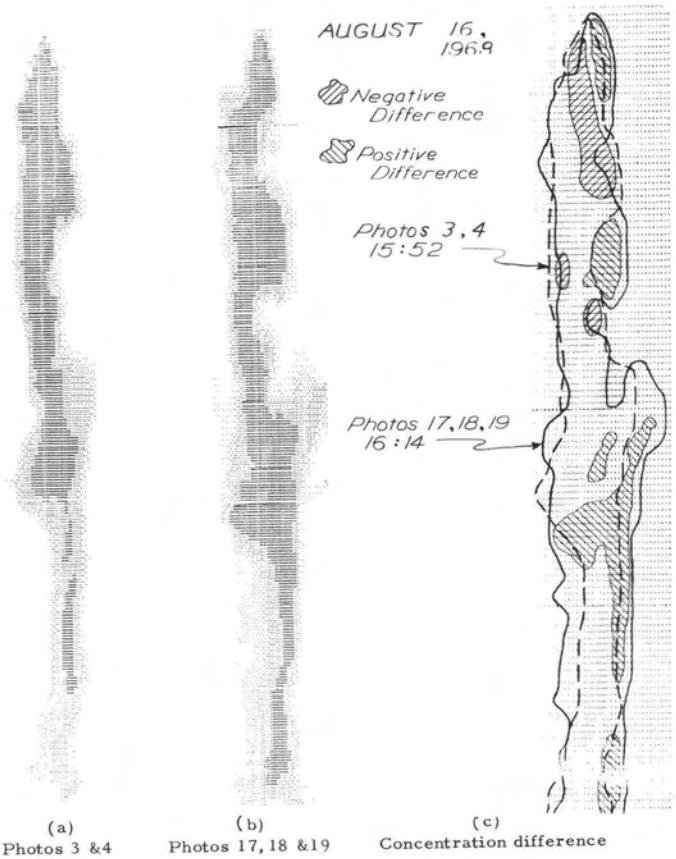

FIG. 8. Waste concentrations determined from aerial photography August 16, 1968. (*a*) Photos 3 and 4. (*b*) Photos 17, 18 and 19. (*c*) Concentration difference.

concentrations, dispersion processes, and current patterns in the outfall area.

Color photography was used to measure the reflected light from the waste in the sea. A relationship between the image densities of the color photography and the effluent concentration in the waste field was developed.

Field studies were conducted simultaneously through observations of the ocean outfall waste plume by aerial photography and conventional boat sampling. The photographic method was evaluated by comparing the concentrations determined from the photography with those measured by boat sampling.

Correlation coefficients between the boat concentrations and the photo concentrations were about 0.9. The discrepancies between the two methods are not entirely due to errors in the photographic procedure but also includes movement of the waste plume between the time of boat sampling and the aerial photography. The boat sampling was conducted over a two-hour period and represents a composite of plume patterns during the sampling period.

CONCLUSION

It is realized that in this initial attempt to develop a color aerial photographic analysis technique to measure waste concentration in an ocean outfall, many simplifying assumptions were necessary. Because of these assumptions, the relationship between waste concentration as derived from the photograph and boat concentration measurements is open to criticism. Neverthelses, we have developed a technique and have identified areas which, through additional research, may result in a precise method for determining outfall waste concentrations remotely. In addition, we have shown how such data, once obtained, can be subjected to computer analysis and displays of results generated.

ACKNOWLEDGEMENT

This research is sponsored by the Federal Water Pollution Control Administration (project 16070 ENS) and was conducted with the cooperation of the Georgia Pacific Corporation and the International Paper Company. The authors wish to acknowledge the efforts of the 34 students, staff members and persons from the Pacific Northwest Water Laboratory who have contributed to the project.

REFERENCES

1. Jensen, N., *Optical and Photographic Reconnaissance Systems*. New York, John Wiley and Sons, 1968. 211 p.
2. Jerlov, N. G., *Optical Oceanography*. Amsterdam, Elsevier, 1968, 194 p.
3. Keller, M. and G. C. Tewinkel, Space Resection in Photogrammetry. Washington, D.C., 1966. 9 p. (Coast and Geodetic Survey *Technical Bulletin 32*)
4. Silvestro, F. B. and K. R. Piech, Development of Aerial Photography as an Aid to Water Quality Management. Cornell Aeronautical Laboratory *Final Report* No. VT-2614-0-1. January 1969.
5. Valley, S. L., *Handbook of Geophysics and Space Environments*. Air Force Cambridge Research Laboratories. 1965.

MEASURING & INTERPRETING ENVIRONMENTAL CHANGE

ASP ACSM

1971 CONVENTION
WASHINGTON, D.C.
MARCH 7-12

The 37th Annual Meeting of the American Society of Photogrammetry will be held at the Washington Hilton Hotel, Washington, D.C., March 7-12, 1971 as part of the 1971 ASP-ACSM Convention. The ASP Technical Program will feature papers reflecting recent developments in:

- Photogrammetric Techniques and Instrumentation
- Aerial Photography
- Remote Sensing
- Photo Interpretation
- Analytical Photogrammetry
- Non-Topographic Photogrammetry
- Photogrammetric Applications

For further information write to American Society of Photogrammetry, 105 N. Virginia Ave., Falls Church, Va. 22046.